Field-Scale Mapping of Surface Soil Organic Carbon Using Remotely Sensed Imagery

Feng Chen,* David E. Kissel, Larry T. West, and Wayne Adkins

ABSTRACT

The surface soil organic C (SOC) concentration is a useful soil property to map soils, interpret soil properties, and guide fertilizer and agricultural chemical applications. The objective of this study was to determine whether surface SOC concentrations could be predicted from remotely sensed imagery (an aerial photograph of bare surface soil) of a 115-ha field located in Crisp County, Georgia. The surface SOC concentrations were determined for soil samples taken at 28 field locations. The statistical relationship between surface SOC concentrations and image intensity values in the red, green, and blue bands was fit to a to a logarithm linear equation (R^2 = 0.93). The distribution of the surface SOC concentrations was predicted with two approaches. The first approach was to apply the relationship to individual pixels and then determine the distribution; the second approach was to classify the image and then apply the relationship to determine the class boundaries and means. Eight levels of surface SOC concentrations were classified in both approaches, and there was good agreement between the two approaches with a probability value near one using a paired *t*-test. The predicted and measured surface SOC concentrations, based on additional soil samples from 31 field locations, were compared using linear regression (r^2 = 0.97 and r^2 = 0.98 for the two approaches). The surface SOC concentrations were correctly classified in 77.4 and 74.2% of cases for the two approaches. The procedures tested were accurate enough to be used for precision farming applications in agricultural fields.

Traditionally, farm managers apply fertilizers, chemicals, and other crop-production inputs to optimize the production of the field as a whole. This management protocol often results in over-application of crop-production inputs in some field areas and under-application in others because of variations of field characteristics, including soil organic C, soil texture, soil nutrients, field topography, and other properties. In addition, uniform applications may increase the chances of pollution of the environment due to excess application in some field areas. Precision farming technology has been shown to optimize application rates if the variation of field characteristics can be used to guide the application rate of crop-production inputs (Lowenberg-Deboer and Boehlje, 1996; Rawlins, 1996; Wolf and Buttel, 1996; Joseph 1998). The organic C concentrations of surface soil have been used to spatially vary the application rate of some crop-production inputs (Blackmer and White, 1998). The surface soil organic C concentration affects the activity of many herbicides (Hance, 1988), influences plant-available N (Dahnke and Johnson, 1990), and also affects the soil's ability to adsorb plant nutrients (Havlin et al., 1999). Knowing its concentration may therefore be useful, especially if its spatial distribution could be determined accurately (Blackmer and White, 1998) and for low cost (Wolf and Buttel, 1996; Lu et al., 1997).

The dark color of soil is typically associated with high organic-matter concentration and high native fertility. Soils with thick, dark surface horizons are often separated from other soils at the highest categorical level in many soil classification systems, reflecting the differences in the genesis of soils as well as the importance of these soils as a medium for plant growth and independent natural bodies worthy of further study (Schulze et al., 1993). Research has been done concerning the relationships between soil color and soil organic matter. However, many of these studies were based on Munsell color notations for specific soils at specific locations (Alexander, 1969; Steinhardt and Franzmeier, 1979; Schulze et al., 1993) or for the purpose of designing spectral sensors (Pitts et al., 1983; Griffis, 1985; Smith et al., 1987).

There were attempts to quantify relationships between soil color and organic matter concentrations by Brown and O'Neal in the 1920's (Schulze et al., 1993). Later, color charts or tables that described the relationships between soil color and organic-matter concentration were developed by using visual color descriptions or Munsell soil color charts (Shields et al., 1968; Alexander, 1969; Steinhardt and Franzmeier, 1979). Shields et al. (1968) conducted a study of several Ap horizons in an attempt to distinguish between two soils, based on the soil color. Organic C was found to be correlated with soil color for both soils. Alexander (1969) developed a color chart for visually estimating the organic-matter concentration of Ap horizons from more than 300 Illinois soil samples. Steinhardt and Franzmeier (1979) correlated the organic-matter concentrations with the moist soil color for 262 samples of Ap horizons in Indiana. Both papers classified organic-matter concentrations into quantitative categories using the Munsell Color System as standards, and general relationships were developed for visually estimating organic-matter concentrations. Page (1974) used a color-difference meter to examine 96 soils from the Coastal Plain Region of South Carolina and found a curvilinear relationship between reflectance and percent organic matter in the 0 to 5% range. Research has shown that spectroscopic measurement of soil reflectance can give better accuracy in soil color measurement than visual matching (Schulze et al., 1993; Torrent and Barrón, 1993).

Reflectance in various spectral bands has been correlated with soil properties such as soil organic matter. Spectral sensors were designed to measure soil organic matter based on the relationship between light reflectance and soil organic matter (Pitts et al., 1983; Griffis, 1985; Smith et al., 1987; Shonk et al., 1991). Different

Dep. of Crop and Soil Sci., Univ. of Georgia, Athens, GA 30602. Received 29 Oct. 1998. *Corresponding author (fchen@arches.uga.edu).

Published in Soil Sci. Soc. Am. J. 64:746–753 (2000).

Abbreviations: GPS, global positioning system; SOC, soil organic C.

algorithms were developed to transform the output reflectance to concentration of soil organic matter and soil moisture. Baumgardner et al. (1970) used 197 grid samples for a 25-ha field to correlate the soil organic-matter content to different wavelengths in 12 channels from the visual to infrared range, and a computer printout of soil pattern was generated. It was shown that the organic-matter content can be predicted from light reflectance with a linear or curvilinear relationship in the visual and infrared range (Baumgardner et al., 1970; Leger, 1979; Cihlar et al., 1987; Smith et al., 1987; Sudduth and Hummel, 1988; Shonk et al., 1991; Henderson et al., 1992). Research also showed that the relationship between soil organic matter and reflectance is poor if soil samples were collected from large geographic areas or different landscapes, such as soil samples from an entire state (Fernandez et al., 1988; Henderson et al., 1992; Schulze et al., 1993). The cause may be due to different types of parent materials (Henderson et al., 1992).

In previous research, there was no attempt to accurately determine the distribution of surface soil organic C (SOC) concentrations based on the reflected image intensity data for a field, which may be useful for precision farming. Relatively simple and inexpensive methods that would be both more accurate and less expensive than grid sampling are needed to develop maps of surface SOC concentrations. The method should employ only the minimum number of soil samples for organic C analysis to minimize the costs for creating maps. The objective of this study was to map the surface SOC concentrations for a field using an inexpensive remotely sensed image, a color slide, coupled with image processing and auto-classification technology and statistical approaches. A field located in Crisp County, Georgia, was selected for this study, in part because of its range and spatial distribution of surface SOC concentrations.

MATERIALS AND METHODS

The field selected for this research is located in the northwest corner of Crisp County, Georgia, 83°56′20.510″ to 83°56′51.944″ W; 32°00′16.994″ to 32°01′24.675″ N (Fig. 1). The area of this field is about 115 ha with elevations varying from 75 to 85 m. The field was selected because it is quite variable in surface soil texture and organic matter and is representative of large areas of the Coastal Plain Region in Georgia. An aerial photograph color slide of the entire field with a bare and dry surface was taken by the USDA Farm Service Agency in spring 1997. In December 1997, a total of 28 soil samples were obtained from the field and their locations were measured using a global positioning system (GPS) with submeter accuracy. Areas sampled were based on the variation in the apparent surface soil texture across the field, as well as on a range of soil organic-matter levels within the different textural areas. The soil samples taken at each location consisted of nine soil cores taken randomly from the 0- to 15-cm soil depth within a 2 by 2 m^2 area using a 2-cm diam. oakfield soil probe. These samples were composited and mixed thoroughly for organic C analysis. The soils were taken to the laboratory and air-dried during the next 2 to 3 d, sieved with a 2-mm sieve, and then stored in plastic containers until analyzed. The total SOC concentrations of these samples were

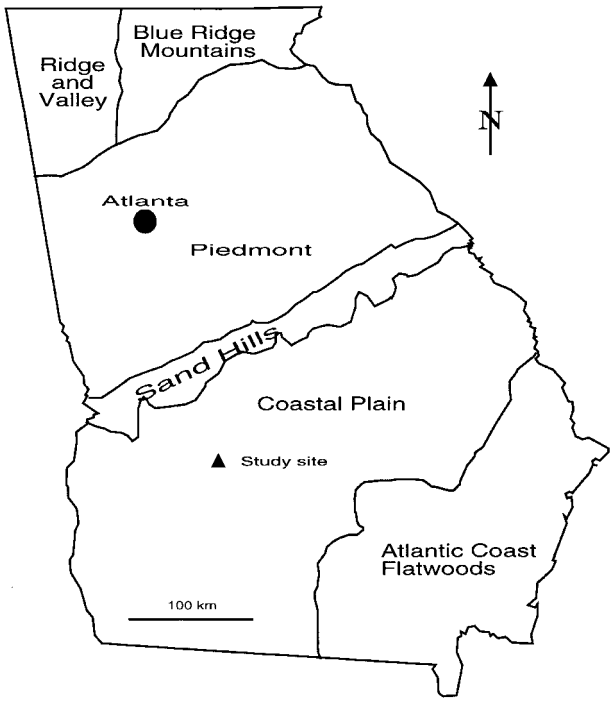

Fig. 1. Location of the study site in Georgia.

determined with a Leco CNS analyzer (Leco, St. Joseph, MI) (Nelson and Sommers, 1996). After the 28 samples were collected, the distribution of image-intensity values at the sampling locations was also observed to determine if the image-intensity values were well distributed. Wide distributions in image-intensity values were observed over the red, green, and blue bands (Fig. 4). These 28 soil samples were used to develop the relationship between surface SOC concentrations and image-intensity values. To verify the relationship, 32 soil samples were obtained from other locations within the same field in March and June 1998. One of these samples was not used because it was too close to a shade tree. The sampling procedures, sample processing, storage, and analysis were the same as for the 28 samples, except that 14 of the samples were the samples from grid sampling on 0.4-ha centers. These 14 samples were selected from relatively uniform areas >0.4 ha. For these samples, nine cores were composited.

The color slide of the field was scanned into the computer with a resolution of 2700 lines per inch. This image was georeferenced into Universal Transverse Mercator projection based on sub-meter GPS measurements of targets, including trees, road intersections, and artificial targets, within and surrounding the field. After rectification, the image was resampled from the scanned pixel size into 2- by 2-m cell resolution. The rectified image was then converted into ASCII format for further processing (classifying) the image. Because the image was a color image, three arrays (red, green, and blue bands) were created. The accuracy of image rectification was estimated by using the GPS measurement of some significant objects such as land marks, road intersections, and trees at 15 locations within and around the field. A mean error of about 5 m with a maximum error <10 m was obtained for the differences between the true locations (GPS locations) and the responded image locations.

To reduce the variance (noise) among the image pixels caused by micro-topography, film processing, and scanning, a low-pass filter was applied to the image with a mask in 5 by 5 cells before examining the relationships between image-intensity values and surface SOC concentrations. This is an

Fig. 2. The color slide image of the field. (The image was geo-referenced into the Universal Transverse Mercator coordinate system.)

Fig. 3. The low-pass filtered result for the color slide.

average smoothing filter, as follows:

$$P_n(i, j) = \sum_{k=i+2}^{i+2} \sum_{l=j+2}^{j+2} [W(k, l) \times P_o(k, l)] \qquad [1]$$

where $P_n(i, j)$ is the pixel value for the smoothed image at location (i, j); $P_o(k, l)$ is the pixel value for the image-intensity value at location (k, l); $W(k, l)$ is the weight factor with each W having a value of 0.04; and the range of k is $(i - 2, i + 2)$, the range of l is $(j - 2, j + 2)$.

Based on the locations for the 28 soil samples, the pixel values of these 28 locations were determined from the filtered image. The relationship between surface SOC concentrations and the pixel values for the 28 samples was developed by regression analysis. This relationship was applied to the original image, and then an image representing the distribution of surface SOC concentrations for the field was obtained. The result was called *Pre_Result1*. The filtered image was not used in this case because smoothing would remove real spatial variability in surface SOC concentrations.

An alternative approach was also used to perform a classification to the original image by a minimum-distance clustering algorithm (Jensen, 1986; Lillesand and Kiefer, 1987). This algorithm uses minimum spectral distance to assign a cluster (class) for each candidate pixel. The process begins with an arbitrary number of clusters (classes), and then it processes repetitively until meeting a certain stop condition (or conditions). The input parameters for the method include: (i) the maximum number of clusters to be considered (N); (ii) the convergence threshold (T), which is the maximum percentage of pixels whose class values are allowed to be unchanged between iterations; and (iii) the maximum number of iterations (M).

The process of this algorithm is as follows: (i) Arbitrarily initialize the mean for each of N clusters by simply dividing the image into N groups and then computing the mean for each group. (ii) For each pixel, compute the spectral distance between this pixel and each cluster mean, and assign the pixel to the cluster with the minimum distance between the cluster mean and the pixel. This process is repeated until the percentage of unchanged pixels is greater than or equals T, or the number of iterations is greater than or equals M. In each iteration, the mean of each cluster is recomputed, and these new means will be used for the next iteration. Initially, 20 classes were developed using this procedure.

The classified result was further processed to identify the surface SOC concentrations for each class based on the relationship between surface SOC concentrations and the pixel intensity values. The procedure was as follows: (i) compute the average image-intensity value and the histogram of image-intensity values for each class based on the original rectified image and the classified result. The image-intensity values of each class were extracted from the original image, whereas the boundary of each class was identified by the classified result; and (ii) determine the average surface SOC concentration and histogram of surface SOC concentrations for each class based on the relationship between surface SOC concentrations and the image-intensity values. The result was called *Pre_Result2*.

Based on the histogram of each class from Pre_Result2, Pre_Result2 was reclassified, and eight classes were derived from the reclassification; the result was referred to as *Result2*. Then according to the class range of Result2, Pre_Result1 was

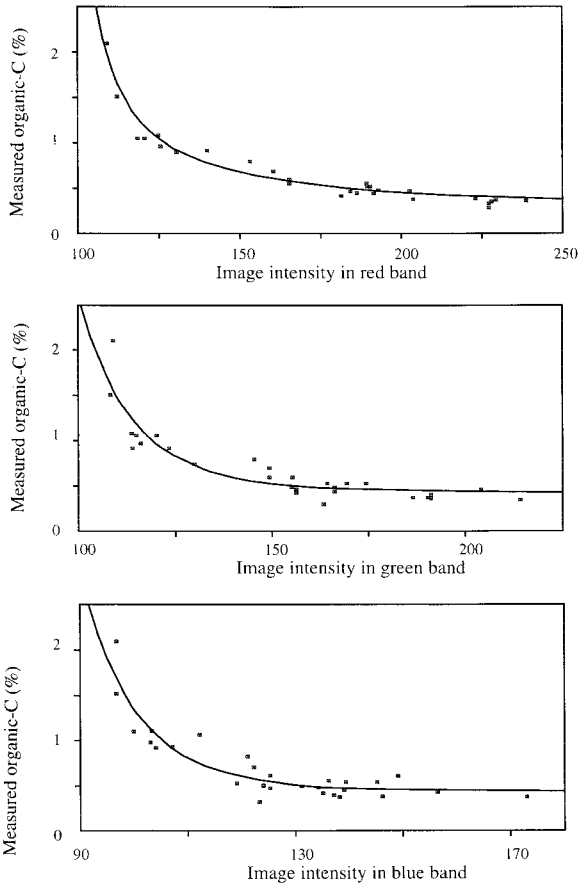

Fig. 4. Plots and the fitted curve between organic-C concentrations and image-intensity value for the red, green, and blue bands. [The fitted equation, with $R^2 = 0.9266$, is log(%SOC) = 1.715 − 0.0158 Red + 0.0128 Green − 0.0113 Blue].

also classified into eight classes; and the result was referred to as *Result1*.

Further processing of the results (Result1 and Result2) was necessary because of two problems: The first was pixel values that were located outside the field; this area needed to be removed (for the reason of statistics and mapping). The second problem was the *single-pixel* classes in the results of the second classification. These single-pixel classes are mainly from *spot* noise in the original slide and scanning process.

The first problem was solved by measuring the field boundary with sub-meter accuracy GPS and discarding pixels outside the measured field boundary.

For the second problem, a majority algorithm was used to filter out single-pixel classes. This method sets a pixel value at location (i, j) to the pixel value that has the majority number in the filter mask. The process is as follows: (i) choose a suitable mask size and move the mask over the image. A mask with 3 by 3 cells was selected because it can effectively remove the single-pixel classes but keep all classes with five or more pixels; (ii) for each pixel at location (i, j), look for the pixel value P_m with the maximum number (majority) in the mask; and (iii) reassign the pixel value at location (i, j) to P_m. The final results were referred as *Post_Result1* and *Post_Result2*. Comparisons between Post_Result1 and Post_Result2 were conducted by examining the area of each class and a histogram representing the degree of difference of uncommon class pixels.

The accuracy of the results obtained above was checked, based on the other 31 soil samples, which were different from

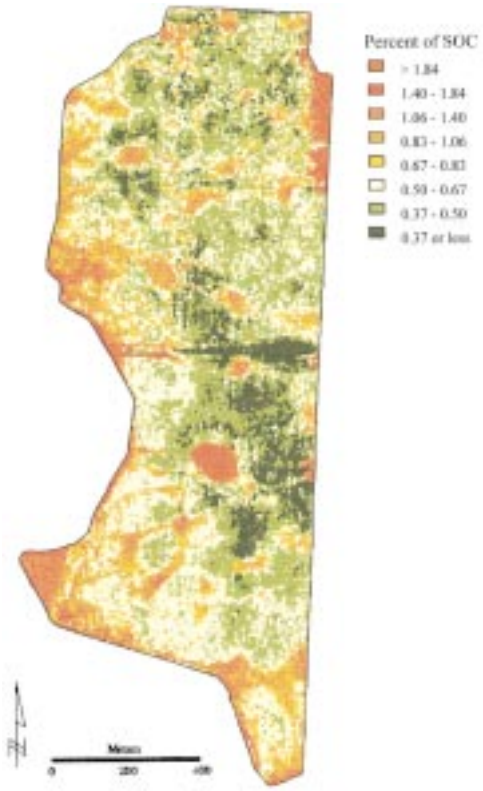

Fig. 5. The result of Post_Result1. (This image was obtained by first examining the organic-C concentrations for each pixel and then classifying the result into eight classes. The clip and majority were applied before final display.)

those samples for model development. The check for each location was based on a point buffer (square buffer) with a buffer size of 5 by 5 pixels (10 by 10 m) to reduce the error caused from image rectification. For each location at (x, y), the buffer, with the center at (x, y), was overlaid on the result image. The average SOC concentrations within this buffer was computed, as follows:

$$\mathrm{SOC}_0(x, y) = \left[\sum_{k=x-2}^{x+2}\sum_{l=y-2}^{y+2} \mathrm{SOC}_i(k, l)\right]/S \qquad [2]$$

where $\mathrm{SOC}_o(x, y)$ is the average SOC concentration over the buffer centered at location (x, y) from the result image; S is the size of the buffer ($S = 25$ for this research); $\mathrm{SOC}_i(k, l)$ is the value of the SOC concentration at location (k, l). This is the average value for a class; and the range of k is $(x - 2, x + 2)$, the range of l is $(y - 2, y + 2)$ in this research.

The measured data and the average value within the buffer were compared to check the accuracy of the final classification results, Post_Result1 and Post_Result2. Two approaches were used to check the accuracy: In the first approach, a relationship between measured and estimated values was developed by a linear regression. The r^2 values were examined for the two methods. In the second approach, the measured and predicted values were classified into one of the eight classes based on the class scheme. For each location, the measured and the predicted surface SOC concentration values were examined to check if they were in the same class.

RESULTS AND DISCUSSION

The geo-referenced image for the field is shown in Fig. 2. On this image, the field is dry without any vegetation

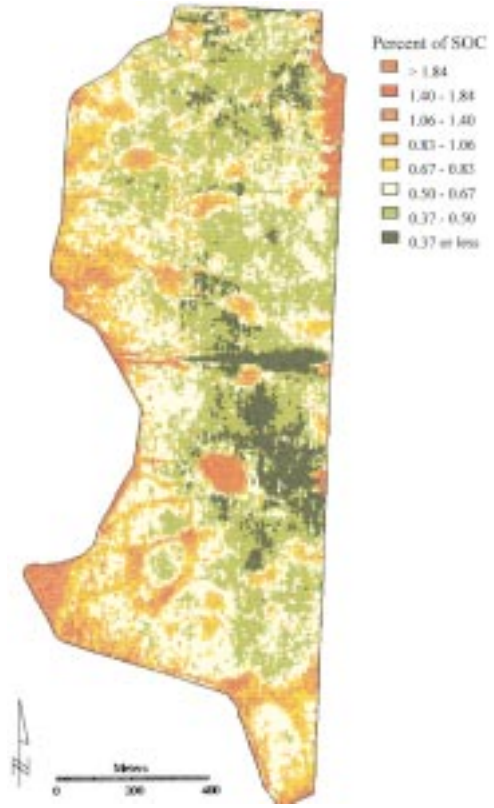

Fig. 6. The result of Post_Result2. (This image was obtained by first classifying the bare surface image into 20 classes, examining the organic-C concentrations with the average, upper-bound, and lower-bound values for each class, and then grouping these 20 classes into 8 classes. The clip and majority were applied before final display.)

cover, so the color represents the surface soil color. In general, dark color areas indicate high SOC concentrations, whereas the light areas indicate low SOC concentrations. Different degrees of red colors may reflect the different levels of Fe concentrations. Shadows existed along the east boundary of the field. However, this was not considered in the data analysis since the shadows only occupied a small area. These shadows can be removed if another photo in which the shadow area is clear is available.

Relationship Between Image-Intensity Values and Organic Carbon Concentrations

To suppress the effect of geo-reference errors on the building of the relationship between the organic-C concentrations and image-intensity values, a low-pass filter was applied and the result is shown in Fig. 3. Using this result and the analyzed data of organic-C concentrations, the relationship between them was examined. The plots of organic-C concentrations vs. the image-intensity values of the three bands (red, green, and blue) are shown in Fig. 4. A logarithmic linear equation was derived from analysis of the plots, as follows:

$$\mathrm{SOC} = \exp(a + bR + cG + dB) \quad (R^2 = 0.9266) \qquad [3]$$

where SOC is the percentage of surface SOC concentration; R, G, and B are the image-intensity values for the red, green, and blue bands; and a, b, c, and d are coefficients where $a = 1.71499$, $b = -0.01576$, $c = 0.01281$, $d = -0.0113$.

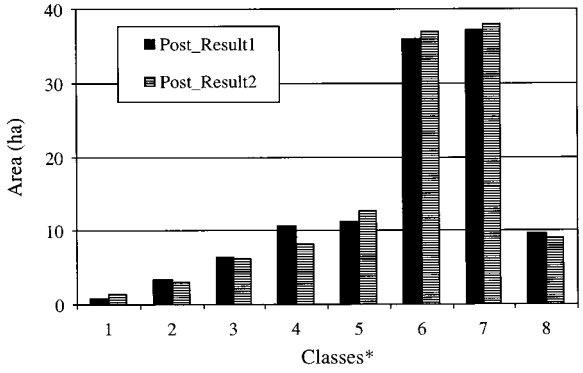

*Class ranges are as follows:

Class	%SOC	Class	%SOC
1	> 1.84	5	0.67 - 0.83
2	1.40 - 1.84	6	0.50 - 0.67
3	1.06 - 1.40	7	0.37 - 0.50
4	0.83 - 1.06	8	0.37 or less

Fig. 7. Area comparison of two approach results, Post_Result1 and Post_Result2.

Classification of Surface Soil Organic-Carbon Concentrations

The relationship was applied to the image with two different methods. In the first method, Eq. [3] was used to calculate the surface SOC concentrations for each pixel with the resulting values grouped into one of eight classes. In the second method, the image was classified into 20 cluster groups, then Eq. [3] was applied to the classified result, and finally the original 20 cluster groups were further grouped into eight classes. Both methods used the same ranges of surface SOC concentration for each class. Comparing these two methods, the result using the first approach illustrates more detailed information but it might also introduce some noise such as from surface micro-topography, whereas the result using the second approach shows information more globally (less detail) but it might miss some true classes.

Table 1. Degree of difference between Post_Result1 and Post_Result2.

Degree of difference†	Percent	Number of pixels
	%	
8	0	0
7	0.0	1
6	0.01	36
5	0.05	158
4	0.14	411
3	0.5	1 328
2	3.3	9 545
1	28.6	82 345
0	67.4	193 948

† The degree of difference indicates the consistency between Post_Result1 and Post_Result2. For example, the degree of difference 0 means that a pixel was classified into the same class in Post_Result1 and Post_Result2; and 1 means that a pixel was classified into different classes in Post_Result1 and Post_Result2 but their class difference is 1 (e.g., a pixel was classified into Class 4 in Post_Result1 while it was classified into Class 5 in Post_Result 2).

It could be found that a significant number of single-pixel classes existed from the above results. These single-pixel classes may show some details about the distribution of surface SOC concentrations. However, the field survey found that most of these details were not the true representation of the field distribution of surface SOC concentrations. In addition, these single-pixel classes caused too much image variance for analyzing and mapping the results. These single-pixel classes needed to be removed, which was done using the majority method. The results were then converted into vector format (classes are represented by polygons rather than by pixels), and a color scheme was applied to them for the output. Figures 5 and 6 show the results by using the first method and the second method respectively, with single-pixel classes removed.

Comparison of Two Approaches

The area for each class from the two classification approaches, Post_Result1 and Post_Result2, were compared and found to be very similar (Fig. 7), based on a paired *t*-test for the area distribution, which gave a value of $P > 0.99$. The common pixel classes were also compared, with 67.4% of the pixels classified in the same classes for the two classification methods (Table 1). For pixels with different classes, 87.7% of them were classified into their neighbor classes; for example, in Post_Result1, a pixel was classified into Class 4 while in Post_Result2, this pixel was classified into Class 5.

Model Validation

The linear relationship between the measured and the predicted surface SOC concentrations are shown in Fig. 8 and 9. For both classification approaches, there was good agreement between the measured (from 31 locations) and the predicted values with an r^2 of 0.98 for Post_Result1 and 0.97 for Post_Result2 at $P < 0.00$ under a 0.95 confidence level. In addition, the statistical analysis showed that the slopes of the linear regression lines were close to 1 (0.9975 and 0.9917) at $P < 0.00$ under a 0.95 confidence level. The intersects ($\neq 0$) were not significant at $P < 0.15$ for Post_Result1 and at $P < 0.45$ for Post_Result2 under a 0.95 confidence level, so they were not considered in the linear equations. From the scatter plots, we also noted that the prediction of the surface SOC concentrations <1.3% was better than that of the surface SOC concentrations >1.3%.

The classification accuracy was also evaluated by checking whether the measured and the predicted classes were the same class (Table 2). From the check of the 31 locations, the Post_Result1 had seven locations that were classified into wrong classes and the Post_Result2 had eight locations that were classified into wrong classes. Overall, the correctness for Post_Result1 was 77.4% and the correctness for Post_Result2 was 74.2%. When we further examine the misclassified locations, we found that within those misclassified locations, all of the misclassified locations in Post_Result1 and all but two of the misclassified locations in

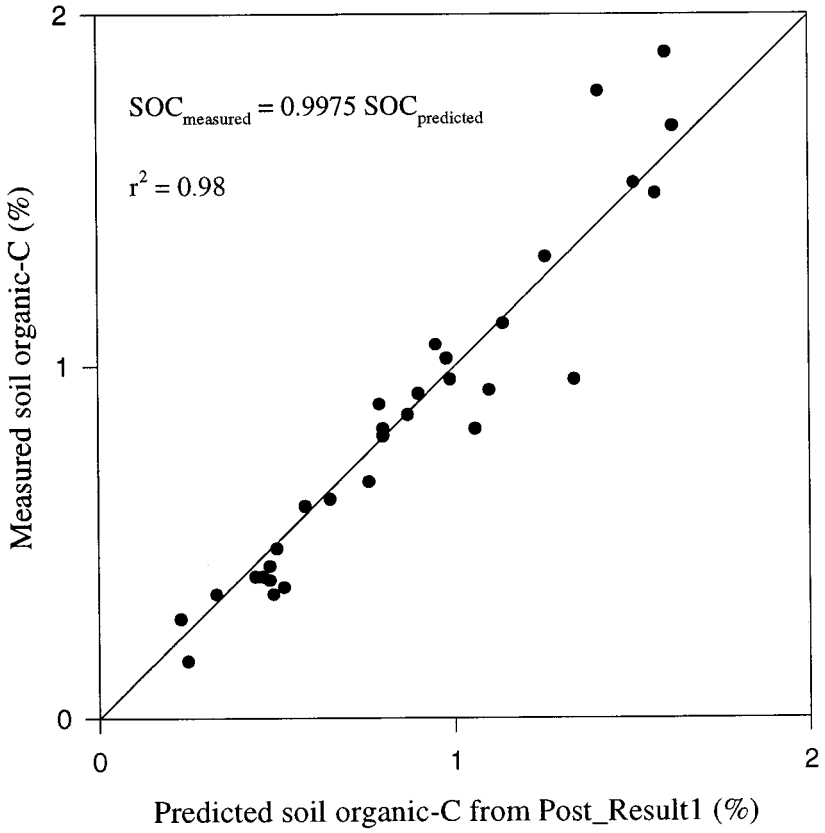

Fig. 8. The linear relationships between measured and predicted (Post_Result1) organic-C concentrations for the 31 locations.

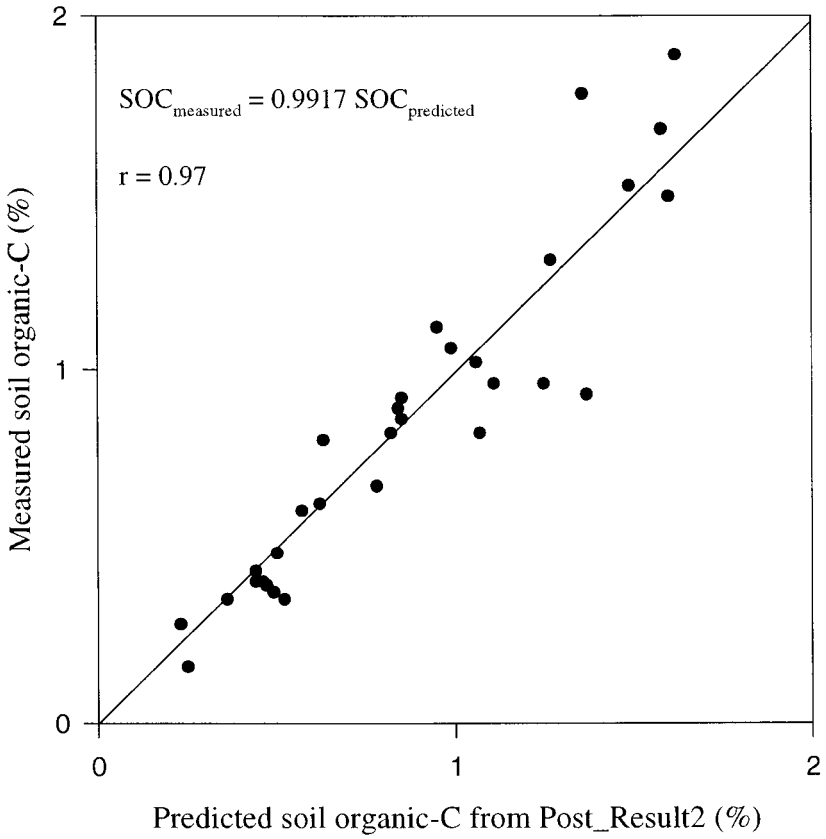

Fig. 9. The linear relationships between measured and predicted (Post_Result2) organic-C concentrations for the 31 locations.

Post_Result2 were placed into their neighboring classes. There might be a trend to the misclassification locations. For the low organic-C locations, the misclassification was more likely classified into its higher organic-C classes; however, for the high organic locations, it was more likely classified into its lower organic-C classes.

Comparison with Grid Sampling

Compared with grid sampling, the primary advantage of the method in this paper lies in its low cost as well as the detailed and accurate description of spatial variation in mapping soil organic matter. With grid sampling, eight to ten cores are typically taken for a composite sample to represent a 0.405-ha (1-acre) or larger area. This procedure may miss some high or low areas of organic C within the acre. Even if the individual core samples adequately represent the area sampled, the composite sample will not allow one to describe the variation within the area of the composite sample, in this case, an area 64 by 64 m. For the method described here, the image pixel size was 2 by 2 m, allowing the mapping of the distribution of surface SOC concentrations at this resolution.

In addition, the methods developed in this research would have other advantages compared with grid sampling. At present, grid sampling for precision farming is labor-intensive and expensive both for soil sampling and for analysis. For example, 280 samples, based on a 0.405-ha (1-acre) grid size, would be taken in this field if the grid sampling method is used. For the method described in this paper, the number of samples (for developing the relationship between surface SOC concentrations and image-intensity values) was reduced to 28, which would be 10% of the number required to grid sample at a scale of 0.405 ha.

SUMMARY

In summary, we found that high-resolution, remotely sensed imagery of a bare soil field could be quantified to describe the spatial variation of the organic-C concentrations of surface soil for a field in southwest Georgia. The technology and methodology were simple and accurate enough to be of practical use in agricultural production fields. They are also less expensive and more accurate than traditional methods for developing maps of soil organic matter that employ grid sampling, soil analysis, and spatial statistics to develop maps. The relationship between reflected radiation in the visible range and organic C of a bare soil field developed in this research, perhaps with some modifications, might be applied in other fields in the southeast Coastal Plain Region. We will examine other fields in the near future for this purpose.

For further refinement, there are two things we may need to consider for use in other fields in the region. The first is the effect of noise from other soil properties, such as the soil Fe concentration. However, Fe concentration was as high as 1.2% in the original data and 1.1% in the test data and appeared to create no problems.

Table 2. Correctness of classification results for Post_Result1 and Post_Result2.

Location no.	True class	Post_Result1	Post_Result2	Incorrect†
29	7	7	7	
30	7	7	7	
31	6	6	6	
32	4	4	4	
33	7	7	7	
76	7	7	7	
117	7	7	7	
198	7	6	7	01
218	8	8	8	
224	5	4	3	00
228	8	7	6	00
246	5	5	6	10
248	4	4	4	
254	6	6	6	
257	4	4	4	
273	7	7	7	
274	2	2	2	
281	4	4	4	
282	6	5	4	00
1002	5	5	5	
1003	4	3	3	00
1004	2	2	3	10
1005	3	3	4	10
1006	4	4	4	
1007	8	8	8	
1008	8	8	8	
1009	2	2	2	
1010	3	3	3	
1011	1	2	2	00
1012	4	5	4	01
1013	2	2	2	

Class ranges are as follows:

Class	%SOC	Class	%SOC
1	>1.84	5	0.67–0.83
2	1.40–1.84	6	0.50–0.67
3	1.06–1.40	7	0.37–0.50
4	0.83–1.06	8	0.37 or less

† 00: both classes from Post_Result1 and Post_Result2 were incorrect.
01: class from Post_Result1 was incorrect.
10: class from Post_Result2 was incorrect.

Therefore, we concluded that the effect of Fe was not significant for predicting organic-C concentrations in this field. However, the effect of Fe concentrations may need to be considered in other fields because of its importance, either as variables in regression analysis or removing the effect of Fe concentration from the original image before the organic-C concentration analysis.

Another issue we may need to consider is the consistency of image-intensity values. In this study, we used a color slide as the source image. The lighting conditions at the time a photograph is taken and the development processing of slide film both may vary from one field to another and the scanning of color slides may change the true radiated values and may introduce noise. To avoid or minimize these sources of errors, a digital multispectral image could be used as the source image of a field. With digital imagery, the spectral radiance from surface objects is directly recorded and saved in image files and does not require a processing step that can vary from one image capture to another. Data from digital imagery could be more consistent and avoid the effects of variable lighting and processing associated with film development and scanning.

REFERENCES

Alexander, J.D. 1969. A color chart for organic matter. Crop Soils 21:15–17.

Baumgardner, M.F., S. Kristof, C.J. Johannsen, and A. Zachary. 1970. Effects of organic matter on the multispectral properties of soils. Indiana Acad. Sci. 79:413–422.

Blackmer, A.M., and S.E. White. 1998. Using precision farming technologies to improve management of soil and fertilizer nitrogen. Aust. J. Agric. Res. 49:555–564.

Cihlar, J., R. Protz, and C. Prévost. 1987. Soil erosion assessment using remotely sensed data. p. 395–408. *In* P.J. Howarth (ed.) 11th Can. Symp. Remote Sensing, Univ. Waterloo. 22–25 June 1987. Waterloo, Ontario, Canada. Can. Aeronautics Space Inst., Ottawa.

Dahnke, W.C., and G.V. Johnson. 1990. Testing soils for available nitrogen. p. 127–139. *In* R.L. Westerman (ed.) Soil testing and plant analysis. 3rd ed. SSSA Book Ser. 3. SSSA, Madison, WI.

Fernandez, R.N., D.G. Schulze, D.L. Coffin, and G.E. Van Scoyoc. 1988. Color, organic matter, and pesticide adsorption relationships in a soil landscape. Soil Sci. Soc. Am. J. 52:1023–1026.

Griffis, C.L. 1985. Electronic sensing of soil organic matter. Trans. ASAE 28:703–705.

Hance, R.J. 1988. Adsorption and bioavailability. p. 1–19. *In* R. Grover (ed.) Environmental chemistry of herbicides. Vol. 1. CRC Press, Boca Raton, FL.

Havlin, J.L., J.D. Beaton, S.L. Tisdale, and W.L. Nelson. 1999. Soil fertility and fertilizers: An introduction to nutrient management. Prentice Hall, Upper Saddle River, NJ.

Henderson, T.L., M.F. Baumgardner, D.P. Franzeier, D.E. Stott, and D.C. Coster. 1992. High dimensional reflectance analysis of soil organic matter. Soil Sci. Soc. Am. J. 56:865–872.

Jensen, J.R. 1986. Introductory digital image processing: A remote sensing perspective. Prentice-Hall, Englewood Cliffs, NJ.

Joseph, K.B. 1998. Who's minding the farm? GIS World 11(2):46–51.

Leger, K.D., G.J.F. Millette, and S. Chomchan. 1979. The effects of organic matter, iron oxides and moisture on the color of two agricultural soils of Quebec. Can. J. Soil Sci. 59:99–105.

Lillesand, T.M., and R.W. Kiefer. 1987. Remote Sensing and image interpretation. 2nd ed. John Wiley & Sons, New York.

Lowerberg-DeBoer, J., and M. Boehlje. 1996. Revolution, evolution or dead-end: Economic perspectives on precision agriculture. p. 923–944. *In* P.C. Robert et al. (ed.) Proc. 3rd Int. Conf. Precision Agric., Minneapolis, MN. 23–26 June 1996. ASA, CSSA, and SSSA, Madison, WI.

Lu, Y.C., C. Daughtry, G. Hart, and B. Watkins. 1997. The current state of precision farming. Food Rev. Int. 13:141–162.

Nelson, D.W., and L.E. Sommers. 1996. Total carbon, organic carbon, and organic matter. p. 961–1010. *In* R.W. Weaver et al. (ed.) Methods of soil analysis. Part 3. SSSA Book Ser. 5. SSSA, Madison, WI.

Page, N.R. 1974. Estimation of organic matter in Atlantic Coastal Plain Soils with a color difference meter. Agron. J. 66:652–653.

Pitts, M.J., J.W. Hummel, and B.J. Butler. 1983. Sensors utilizing light reflection to measure soil organic matter. ASAE Paper 83-1011. ASAE, St. Joseph, MI.

Rawlins, S.L. 1996. Moving from precision to prescription farming: The next plateau. p. 283–302. *In* P.C. Robert et al. (ed.) Proc. 3rd Int. Conf. Precision Agric., Minneapolis, MN. 23–26 June 1996. ASA, CSSA, and SSSA, Madison, WI.

Schulze, D.G., J.L. Nagel, G.E. Van Scoyoc, T.L. Henderson, M.F. Baumgardner, and D.E. Stott. 1993. Significance of organic matter in determining soil colors. p. 71–90. *In* J.M. Bigham and E.J. Ciolkosz (ed.) Soil color. SSSA Spec. Publ. 31. SSSA, Madison, WI.

Shields, J.A., E.A. Paul, R.J. St. Amaud, and W.K. Head. 1968. Spectrophotometric measurement of soil color and its relationship to organic matter content. Can. J. Soil Sci. 48:271–280.

Shonk, J.L., L.D. Gaultney, D.G. Schulze, and G.E. Van Scoyoc. 1991. Spectroscopic sensing of soil organic matter content. Tran. ASAE 34:1978–1984.

Smith, D.L., C.R. Worner, and J.W. Hummel. 1987. Soil spectral reflectance relationship to organic matter content. ASAE Paper 87-1608. ASAE, St. Joseph, MI.

Steinhardt, G.C., and D.P. Franzmeier. 1979. Comparison of organic matter content with soil color for silt loam soils of Indiana. Commun. Soil Sci. Plant Anal. 10:1271–1277.

Sudduth, K.A., and J.W. Hummel. 1988. Optimal signal processing for soil organic matter determination. ASAE Paper 88–7004. ASAE, St. Joseph, MI.

Torrent, J., and V. Barrón. 1993. Laboratory measurement of soil color: theory and practice. p. 21–33. *In* J.M. Bigham and E.J. Ciolkosz (ed.) Soil color. SSSA Spec. Publ. 31. SSSA, Madison, WI.

Wolf, S.A., and F.H. Buttel. 1996. The political economy of precision farming. Am. J. Agr. Econ. 78:1269–1274.